Supporting Information

Phase transitions and dielectric properties of a hexagonal ABX_3 perovskite-type organic–inorganic hybrid compound: $[C_3H_4NS][CdBr_3]$

Wei-Qiang Liao, Heng-Yun Ye, Yi Zhang* and Ren-Gen Xiong*

Ordered Matter Science Research Center, Southeast University, Nanjing 211189, PR China

*E-mail: xiongrg@seu.edu.cn; yizhang1980@seu.edu.cn.

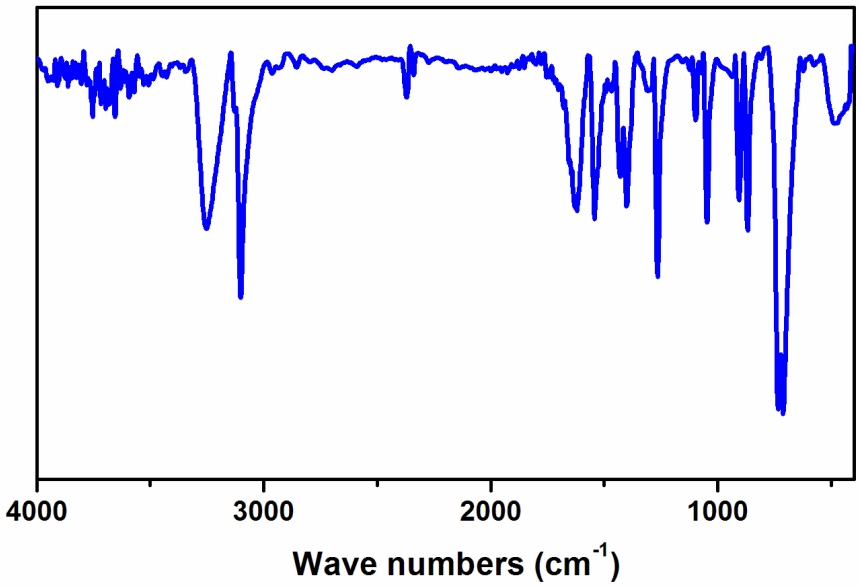

Fig. S1 Infrared (IR) spectra of solid **1** in KBr pellet recorded on a Shimadzu model IR-60 spectrometer at room temperature.

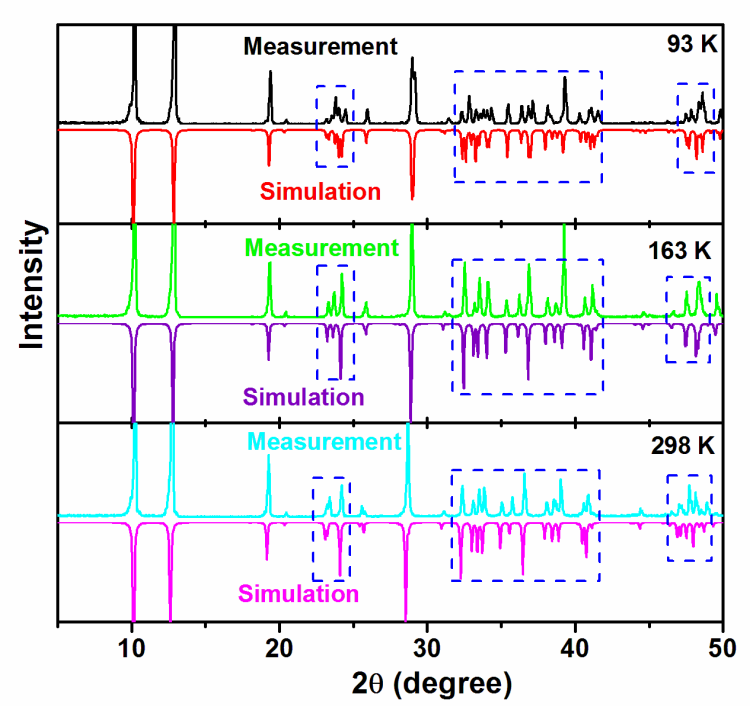

Fig. S2 Experimental powder diffraction (XRPD) patterns matching very well with the simulated ones in terms of the crystal structures for different phases.

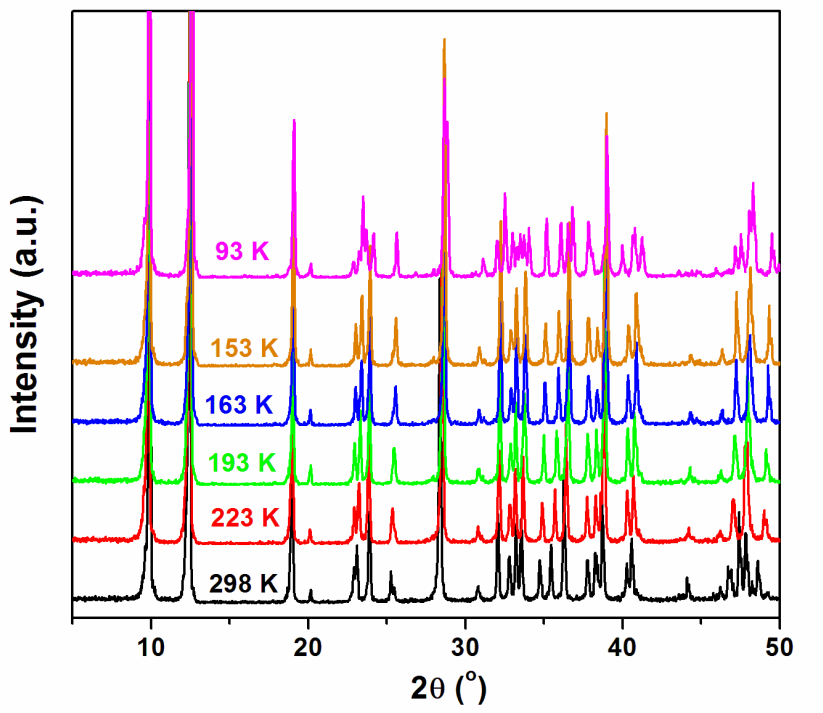

Fig. S3 Variable-temperature XRPD patterns of **1** at selected temperatures.

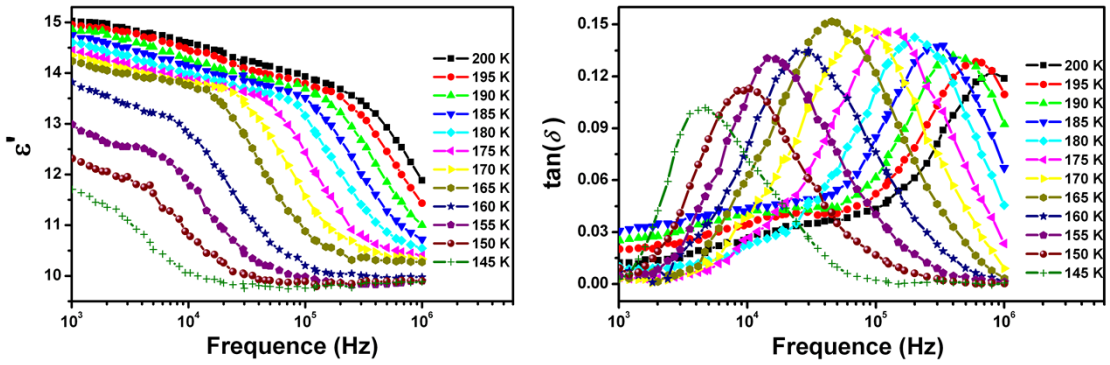

Fig. S4 Frequency dependences of the real part (left) and dielectric loss (right) of the complex dielectric permittivity measured on the single-crystal sample along the *c* axis in the temperature region 145–200 K on cooling.

Table S1. Selected bond lengths [Å] and angles [°] for **1**[a] at 298, 163 and 93 K.

298 K	Cd1–Br1	2.784(10)	Cd1–Br2	2.779(7)
	Br1–Cd1–Br2	84.89(2)	Br1–Cd1–Br2^{i}	95.11(2)
	Br2–Cd1–Br2^{ii}	93.78(3)	Br2–Cd1–Br2^{iii}	86.22(3)
	Br1–Cd1–Br1^{i}	180.00(4)	Br2–Cd1–Br2^{i}	180.00(4)
163 K	Cd1–Br1	2.777(2)	Cd1–Br2	2.771(2)
	Br1–Cd1–Br2	85.21(6)	Br1–Cd1–Br2^{iv}	94.79(6)
	Br2–Cd1–Br2^{v}	93.81(8)	Br2–Cd1–Br2^{vi}	86.19(8)
	Br1–Cd1–Br1^{iv}	180.00(4)	Br2–Cd1–Br2^{iv}	180.00(4)
93 K	Cd1–Br1	2.760(4)	Cd2–Br1	2.773(4)
	Cd1–Br2	2.786(5)	Cd2–Br2^{vii}	2.770(5)
	Br1–Cd1–Br2	94.81(14)	Br1–Cd1–Br2^{vii}	85.19(14)
	Br1–Cd1–Br1^{vii}	93.71(18)	Br1–Cd1–Br1^{viii}	86.29(18)
	Br2–Cd1–Br2^{vii}	180.00(4)	Br1–Cd1–Br1^{ix}	180.00(5)
	Br1–Cd2–Br2^{vii}	85.25(14)	Br1–Cd2–Br2^{x}	94.75(14)
	Br1–Cd2–Br1^{viii}	85.78(18)	Br1–Cd2–Br1^{xi}	94.22(18)
	Br2^{vii}–Cd2–Br2^{x}	180.00(4)	Br1–Cd2–Br1^{xii}	180.00(6)

[a]Symmetry codes:
(i) $-x + 2, -y, z - 1/2$; (ii) $x, -y, -z$; (iii) $-x + 2, y, -z + 1/2$; (iv) $-x + 1, -y + 1, z - 1/2$; (v) $x, -y + 1, -z$; (vi) $-x + 1, y, -z + 1/2$; (vii) $-x, y, -z + 1$; (viii) $x, -y, z$; (ix) $-x, -y, -z + 1$; (x) $x, y, z - 1$; (xi) $-x, y, -z$; (xii) $-x, -y, -z$.

Table S2. Hydrogen-Bond Geometry (**Å**, deg) for the weak N–H···Br and C–H···Br interactions at 298, 163 and 93 K in **1**[b].

	D–H···A	H···A	D···A	D–H···A
298 K	N1–H1B···Br1^{i}	3.18	3.8885	137.0
	C2–H2A···Br2^{ii}	3.07	3.6242	118.5
	C2–H2B···Br2^{ii}	2.99	3.6242	124.3
163 K	N1–H1B···Br1^{iii}	3.06	3.7586	135.7
	C2–H2A···Br2^{iv}	3.00	3.5526	118.4
	C2–H2B···Br2^{iv}	2.94	3.5526	122.8
93 K	N1–H1B···Br2	3.12	3.8325	137.5
	N2–H2B···Br2^{v}	3.10	3.7753	132.8
	C2–H2A···Br1^{vi}	2.85	3.4626	122.7
	C2–H2C···Br1^{vi}	2.90	3.4626	118.4
	C3–H3A···Br1^{vii}	3.04	3.5930	117.4
	C3–H3B···Br1^{vii}	2.99	3.5930	122.0

[b]Symmetry codes:
(i) $x - 1/2, y + 1/2, z + 1$; (ii) $x, y + 1, z + 1$; (iii) $x, y, z + 1$; (iv) $-x + 1/2, y + 1/2, -z + 3/2$; (v) $x, y, z - 1$; (vi) $-x + 1/2, y - 1/2, -z + 1$; (vii) $-x + 1/2, y - 1/2, -z$.